The Journal of Immunology

Platelet-Activating Factor Production in the Spinal Cord of Experimental Allergic Encephalomyelitis Mice via the Group IVA Cytosolic Phospholipase A $_2$-Lyso-PAFAT Axis

Yasuyuki Kihara, Keisuke Yanagida, Kayo Masago, Yoshihiro Kita, Daisuke Hishikawa, Hideo Shindou, Satoshi Ishii and Takao Shimizu

J Immunol 2008; 181:5008-5014; ;
doi: 10.4049/jimmunol.181.7.5008
http://www.jimmunol.org/content/181/7/5008

The Journal of Immunology is published twice each month by
The American Association of Immunologists, Inc.,
1451 Rockville Pike, Suite 650, Rockville, MD 20852

Print ISSN: 0022-1767 Online ISSN: 1550-6606.

Platelet-Activating Factor Production in the Spinal Cord of Experimental Allergic Encephalomyelitis Mice via the Group IVA Cytosolic Phospholipase A_2-Lyso-PAFAT Axis[1]

Yasuyuki Kihara,* Keisuke Yanagida,* Kayo Masago,* Yoshihiro Kita,* Daisuke Hishikawa,* Hideo Shindou,* Satoshi Ishii,*† and Takao Shimizu[2]*

Platelet-activating factor (PAF; 1-*O*-alkyl-2-acetyl-*sn*-glycero-3-phosphocholine) plays a critical role in inflammatory disorders including experimental allergic encephalomyelitis (EAE), an animal model for multiple sclerosis (MS). Although PAF accumulation in the spinal cord (SC) of EAE mice and cerebrospinal fluid of MS patients has been reported, little is known about the metabolic processing of PAF in these diseases. In this study, we demonstrate that the activities of phospholipase A_2 (PLA_2) and acetyl-CoA:lyso-PAF acetyltransferase (LysoPAFAT) are elevated in the SC of EAE mice on a C57BL/6 genetic background compared with those of naive mice and correlate with disease severity. Correspondingly, levels of groups IVA, IVB, and IVF cytosolic PLA_2s, group V secretory PLA_2, and LysoPAFAT transcripts are up-regulated in the SC of EAE mice. PAF acetylhydrolase activity is unchanged during the disease course. In addition, we show that LysoPAFAT mRNA and protein are predominantly expressed in microglia. Considering the substrate specificity and involvement of PAF production, group IVA cytosolic PLA_2 is likely to be responsible for the increased PLA_2 activity. These data suggest that PAF accumulation in the SC of EAE mice is profoundly dependent on the group IVA cytosolic PLA_2/LysoPAFAT axis present in the infiltrating macrophages and activated microglia. ***The Journal of Immunology,*** **2008, 181: 5008–5014.**

Platelet-activating factor (PAF[3]; 1-*O*-alkyl-2-acetyl-*sn*-glycero-3-phosphocholine), a potent proinflammatory lipid mediator (1), is believed to be synthesized via two distinct pathways, the de novo and remodeling pathways (Ref. 2 and see Fig. 1). The latter pathway is primarily involved in the synthesis of PAF by stimulated inflammatory cells such as murine peritoneal cells (3, 4) and human granulocytes (5). The initiation of the remodeling pathway requires membrane phospholipid hydrolysis by phospholipase A_2s (PLA_2; EC 3.1.1.4) that supply lyso-PAF, a precursor of PAF. Acetyl-CoA:lyso-PAF acetyltransferase (LysoPAFAT; EC 2.3.1.67) converts lyso-PAF into PAF. PAF activates the PAF receptor (PAFR), a member of the superfamily of G protein-coupled receptors (6), and elicits a variety of biological responses (1). PAF is rapidly degraded by PAF acetylhydrolases (PAF-AH; EC 3.1.1.47) that cleave the acetyl group at the *sn*-2 position to reform lyso-PAF (7).

PLA_2 are classified into three groups: group VI calcium-independent PLA_2s ($iPLA_2$s), secretory PLA_2s ($sPLA_2$s), and group IV cytosolic PLA_2s ($cPLA_2$) (8). Group IVA $cPLA_2$ preferentially liberates arachidonic acid from 2-arachidonoyl-phospholipids (8, 9). The released arachidonic acids are in turn converted into PGs and leukotrienes via the arachidonic acid cascade (10). It is thought that group VI $iPLA_2$ and some types of $sPLA_2$s have the potential to initiate the arachidonic acid cascade, even though these enzymes lack significant substrate specificity (8). Group IVA $cPLA_2$ is also essential for producing PAF, since PAF synthesis is significantly diminished in calcium ionophore-stimulated macrophages derived from group IVA $cPLA_2$-deficient mice as compared with those from wild-type mice (11). Recently, our group has successfully overcome the long-standing challenges of cloning and identifying LysoPAFAT (12), a critical enzyme that produces PAF. We termed the enzyme LsoPAFAT/LPCAT2 (lysophosphatidylcholine acyltransferase 2) (12). We have demonstrated that murine macrophages and neutrophils express LysoPAFAT/LPCAT2 mRNA and possess a LysoPAFAT activity (3, 12). Furthermore, LysoPAFAT/LPCAT2 mRNA is induced by the ligands for TLRs 4 and 9 in murine macrophages (12). These results imply that LysoPAFAT plays a crucial role in the enhanced PAF production in inflammatory disorders.

Multiple sclerosis (MS) is considered to be a $CD4^+$ T cell-mediated autoimmune disease and is characterized by inflammation and demyelination in the CNS (13). The mechanism of MS,

*Department of Biochemistry and Molecular Biology, Faculty of Medicine, University of Tokyo, Tokyo, Japan; and †Precursory Research for Embryonic Science and Technology of Japan Science and Technology Agency, Tokyo, Japan

Received for publication October 9, 2007. Accepted for publication July 21, 2008.

The costs of publication of this article were defrayed in part by the payment of page charges. This article must therefore be hereby marked *advertisement* in accordance with 18 U.S.C. Section 1734 solely to indicate this fact.

[1] This work was supported, in part, by Grants-in-Aid from the Ministry of Education, Science, Culture, Sports and Technology of Japan (to T. S. and S. I.), a grant to the Respiratory Failure Research Group from the Ministry of Health, Labour and Welfare, Japan (to S. I.), Grants-in-Aid for Comprehensive Research on Aging and Health from the Ministry of Health, Labour and Welfare, Japan (to S. I.), the Kato Memorial Trust for Nambyo Research (to S. I.), and the Japanese Society for the Promotion of Science (research fellowships to Y.Ki., D.H., and K.Y.). H.S., S.I., and T.S. were supported by the Center for NanoBio Integration (University of Tokyo).

[2] Address correspondence and reprint requests to Dr. Takao Shimizu, Department of Biochemistry and Molecular Biology, Faculty of Medicine, University of Tokyo, 7-3-1 Hongo, Bunkyo, Tokyo 113-0033, Japan. E-mail address: tshimizu@m.u-tokyo.ac.jp

[3] Abbreviations used in this paper: PAF, platelet-activating factor; PLA_2, phospholipase A_2; LysoPAFAT, acetyl-CoA:lyso-PAF acetyltransferase; LysoPAFAT/LPCAT2, LysoPAFAT/lysophosphatidylcholine acyltransferase 2; lyso-PAF, 1-*O*-alkyl-*sn*-glycero-3-phosphocholine; PAFR, PAF receptor; PAF-AH, PAF acetylhydrolase; PC, phosphatidylcholine; $iPLA_2$, calcium-independent PLA_2; $sPLA_2$, secretory PLA_2; $cPLA_2$, cytosolic PLA_2; MS, multiple sclerosis; EAE, experimental allergic encephalomyelitis; MOG, myelin oligodendrocyte glycoprotein; SC, spinal cord; ESI-MS/MS, electrospray ionization-tandem mass spectrometry; LPCAT1, lysophosphatidylcholine acyltransferase 1; APMSF, amidinophenylmethanesulfonyl fluoride; GFAP, glial fibrillary acidic protein.

however, remains obscure because of limited access to the CNS at various phases of MS. An animal model, experimental allergic encephalomyelitis (EAE), is indispensable for a better understanding of MS pathology (14). Howat et al. (15) suggested an involvement of PAF in EAE for the first time. We have found that PAFR-KO mice immunized with myelin oligodendrocyte glycoprotein (MOG) peptide 35–55 ($MOG_{35–55}$) show less severe symptoms than wild-type mice (16). Group IVA $cPLA_2$ deficiency protects mice from EAE pathology (17). We also have reported that there is a correlation between the PAF level in the spinal cord (SC) and EAE symptoms (16), which is consistent with PAF levels in the cerebrospinal fluid of relapsing-remitting MS patients (18). In the SC of EAE mice, PAF seems to exist in the nanomolar range, which is adequate to provoke biological responses through the PAFR (6). Moreover, the level of PAFR transcript is up-regulated in MS lesions (19) and the CNS of EAE-induced SJL and C57BL/6 mice (16, 20). The elevated levels of both PAF and PAFR transcripts probably worsen the MS/EAE pathology. EAE, as an animal model of MS, is useful for understanding the roles of PAF in MS (14), since studies on PAF in MS lesions are in accordance with those in EAE lesions (16, 18–20). However, the metabolic processing of PAF and involvement of LysoPAFAT/LPCAT2 in EAE pathology are largely unknown. In the present study, we have induced EAE in C57BL/6 mice with the $MOG_{35–55}$ peptide and revealed that PAF accumulation in SCs of EAE mice is dependent on the up-regulation of the expression and activities of both group IVA $cPLA_2$ and LysoPAFAT. This is the first report suggesting the involvement of LysoPAFAT/LPCAT2 in the disease models.

Materials and Methods

Induction of EAE

EAE was induced in 8-wk-old C57BL/6 female mice. The maintenance of the facility and the use of animals were in full compliance with the University of Tokyo Ethics Committee for Animal Experiments. $MOG_{35–55}$ (MEVGWYRSPFSRVVHLYRNGK), corresponding to the fragment of mouse MOG from aa 35–55, was synthesized by Sigma-Aldrich. Mice were immunized s.c. in the flank with 300 μg of $MOG_{35–55}$ peptide in 0.1 ml of PBS and 0.1 ml of CFA containing 0.4 mg of *Mycobacterium tuberculosis* (H37Ra; Difco Laboratories) on days 0 and 7 and injected i.p. with 250 ng of pertussis toxin (List Biological Laboratories) on days 0 and 2. Mice were scored as follows: 0, no sign; 0.5, mild loss of tail tone; 1.0, complete loss of tail tone; 1.5, mildly impaired righting reflex; 2.0, abnormal gait and/or impaired righting reflex; 2.5, hind limb paresis; 3.0, hind limb paralysis; 3.5, hind limb paralysis with hind body paresis; 4.0, hind and fore limb paralysis; 4.5, moribund; and 5.0, death. To understand the EAE pathology, we divided the disease course into induction, acute, and chronic phases in accordance with the clinical symptoms as previously described (Ref. 16 and Fig. 2*A*).

Quantification of PAF

PAF and eicosanoid levels were estimated simultaneously as previously described (21, 22). The results of the eicosanoid levels will be published elsewhere (Y. Kihara, S. Ishii, Y. Kita, S. Uematsu, S. Akira, and T. Shimizu, unpublished data). SCs of naive mice and EAE mice were removed on days 12, 19, and 32, frozen immediately with liquid nitrogen, and stored at −80°C until use. The frozen tissues (~100 mg) were powdered with an SK-100 mill (Tokken), and lipids were extracted for 60 min at 4°C with methanol containing deuterium-labeled 16:0 PAF (Cayman Chemical) as an internal standard. The extracts were loaded onto Oasis HLB cartridges (30 mg; Waters) preloaded with methanol and 0.03% (v/v) formic acid/H_2O. The cartridges were washed with 0.03% formic acid/H_2O, 15% (v/v) ethanol, and petroleum ether. Lipids were extracted with 100% methanol and PAF levels were quantified by reversed-phase HPLC electrospray ionization (ESI)-tandem mass spectrometry (MS/MS) as described previously (21, 22).

Quantitative real-time PCR

On days 11–12, 18–19, and 30–31, naive and EAE mice were anesthetized with urethane (1.5 g/kg of body; Sigma-Aldrich) and intracardially perfused with 10 ml of ice-cold PBS. The SCs were removed and total RNA was isolated using an RNeasy Mini Kit (Qiagen). The purity and integrity of total RNA were determined by the absorbance at $A_{260/280}$ and gel electrophoresis, respectively. One microgram of total RNA was reverse-transcribed using SuperScript II (Invitrogen Life Technologies) according to the manufacturer's instructions. The RT^2 Profiler PCR Array System for PLA_2 (groups IVA, IVB, IVC, IVD, IVE, and IVF $cPLA_2$s, groups V and X $sPLA_2$s, and group VI $iPLA_2$) was purchased from SuperArray, and quantitative RT-PCR for these PLA_2 mRNAs was performed with a 7500 Fast Real-Time PCR System (Applied Biosystems). The relative abundance of PLA_2 mRNA levels in EAE mice compared with naive mice was calculated by the comparative cycle threshold method using hypoxanthine phosphoribosyltransferase as a normalization control. Quantification of LysoPAFAT, lysophosphatidylcholine acyltransferase 1 (LPCAT1), and β-actin mRNA levels was performed with LightCycler FastStart DNA Master SYBR Green I (Roche) as previously described (12, 23). Results were quantified by using standard curves derived from SCs in the acute phase of EAE.

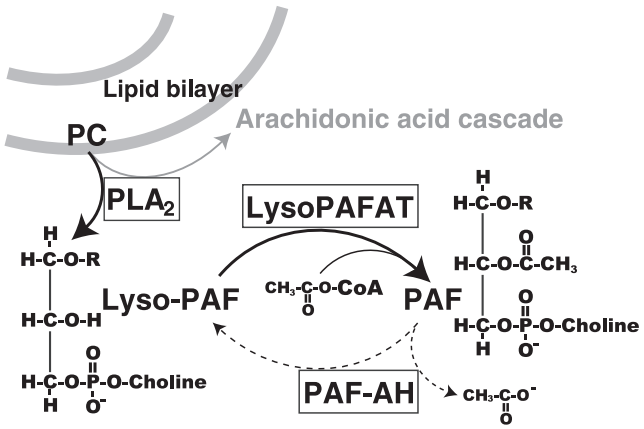

FIGURE 1. PAF production in the remodeling pathway (bold arrow) and degradation pathway (dotted arrow).

Sample preparation for enzyme assays and Western blotting

The SCs of naive mice and EAE mice on days 12, 19, and 34 were removed following perfusion, frozen immediately with liquid nitrogen, and stored at −80°C until use. The tissues (~100 mg) were homogenized with a Physcotoron homogenizer (Microtec) in 500 μl of buffer A (100 mM Tris-HCl (pH 7.4) containing 10.26% sucrose, 20 μM amidinophenylmethanesulfonyl fluoride (APMSF), 5 mM 2-ME, and 1 × Complete Protease Inhibitor Mixture (Roche)). The homogenate was centrifuged at 9,000 × *g* for 10 min at 4°C and the resulting supernatant was centrifuged at 100,000 × *g* for 60 min at 4°C. The pellet was resuspended in buffer B (20 mM Tris-HCl (pH 7.4) containing 20 μM APMSF, 5 mM 2-ME, and EDTA-free 1 × Complete Protease Inhibitor Mixture) and stored at −80°C until use. Protein concentrations were determined by the Bradford method using a protein assay solution (Bio-Rad) and BSA (fraction V, fatty acid-free; Sigma-Aldrich) as a standard.

PLA_2 assay

PLA_2 activity was measured by Dole's method with some modifications (24). Briefly, 5 μg of protein (100,000 × *g* supernatant) was incubated at 37°C for 30 min in a total volume of 0.25 ml of assay buffer (100 mM HEPES-NaOH (pH 7.4) 1 mg/ml BSA, 4 mM $CaCl_2$, and 1 mM DTT) containing mixed micelles (4 μM Triton X-100 and 2 μM 1-palmitoyl-2-[^{14}C]arachidonoyl-phosphatidylcholine (PC) (1.961 GBq/mmol, GE Healthcare BioSciences). The reaction was terminated by adding 1.25 ml of Dole's reagent (isopropanol:*n*-heptane:sulfuric acid, 78:20:2), followed by the sequential addition of 0.75 ml of *n*-heptane and 0.5 ml of water. After centrifugation, an aliquot (0.8 ml) of the upper layer was mixed with 120–150 mg of silica gel, which had been preincubated with 0.75 ml of *n*-heptane. The radioactivity of an aliquot (0.8 ml) was estimated using an LS6500 liquid scintillation counter (Beckman Coulter) in the presence of 1 ml of Microscinti-0 (PerkinElmer).

LysoPAFAT assay

LysoPAFAT activity was measured according to the method of Kume et al. (4, 12, 25), with some modifications. Briefly, 5 μg of protein (100,000 ×

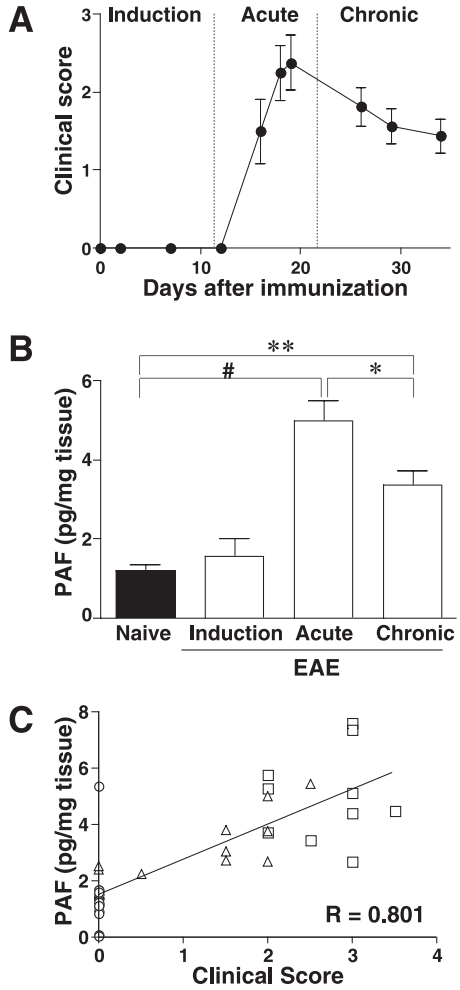

FIGURE 2. Clinical course and PAF levels during EAE. *A*, C57BL/6 female mice were immunized with the $MOG_{35–55}$ peptide. Data are the mean clinical scores ± SEM of eight animals. *B*, PAF levels were determined in SCs of naive mice and EAE mice in the induction, acute, and chronic phases (n = 10 animals). Data represent means ± SEM. #, $p < 0.001$; **, $p < 0.01$; and *, $p < 0.05$ by ANOVA with the Tukey-Kramer test. *C*, PAF levels of naive (●) and EAE mice in the induction (○), acute (□), and chronic (△) phases are positively correlated with the clinical scores ($p < 0.0001$ by the Spearman rank correlation test). Each data point represents the result from a single animal.

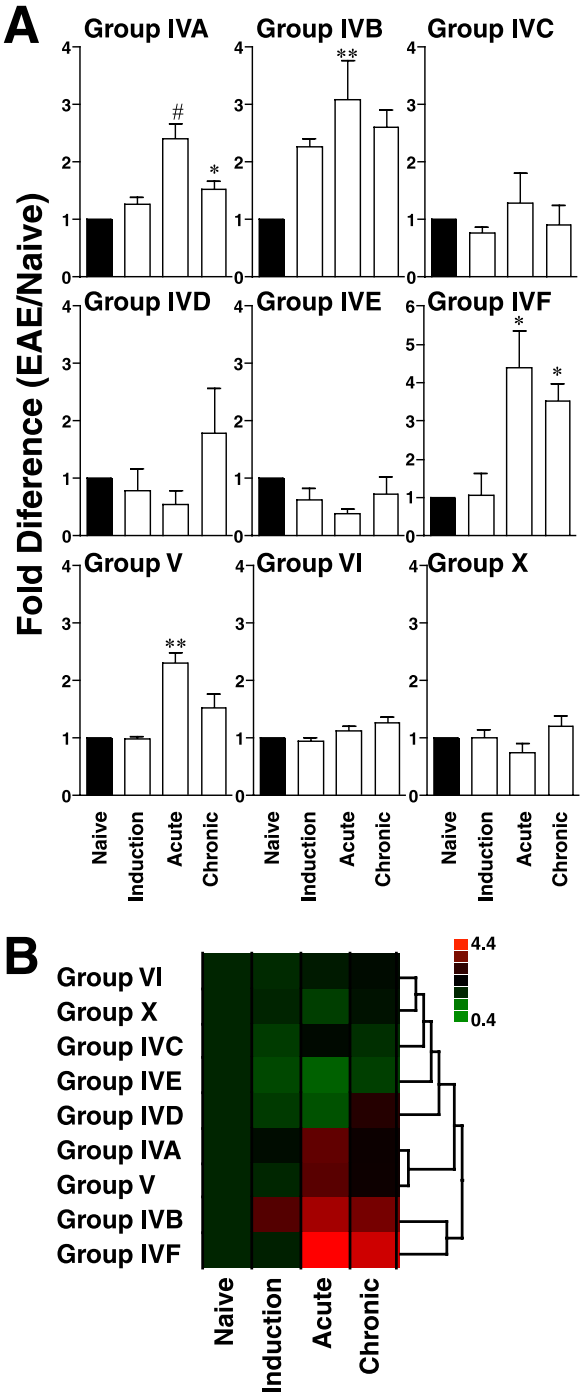

FIGURE 3. PLA_2 mRNA expression in SCs of naive and EAE mice. *A*, Expression of PLA_2 transcripts was quantified by real-time PCR in SCs of naive mice and EAE mice in the induction, acute, and chronic phases (n = 6, 5, 6, and 5 animals, respectively). The relative abundance of PLA_2 mRNA levels in EAE mice compared with naive mice is shown. Data represent means ± SEM. #, $p < 0.001$; **, $p < 0.01$; and *, $p < 0.05$ compared with naive mice by the Kruskal-Wallis test with Dunn's post hoc test. *B*, The relationships among PLA_2 mRNA levels were evaluated by cluster analysis using JMP6 software (Hulinks). The relative expression levels shown in *A* are divided into seven parts and colored from red to green.

g pellet) was incubated at 37°C for 10 min in a total volume of 0.1 ml of reaction mixture (buffer B containing 2 mM $CaCl_2$, 1 mg/ml PC (Sigma-Aldrich), and 100 μM [^{3}H]acetyl-CoA (1.11 GBq/mmol; GE Healthcare BioSciences)) with or without 20 μM lyso-PAF (Cayman Chemical). Subsequently, 122 μl of ice-cold methanol was added to terminate the reaction. The product was bound to 6 mg of C8 resin (Millipore), washed eight times with 55% (v/v) methanol in 20 mM Tris-HCl (pH 7.4), and eluted with 100% methanol. After drying at 50°C for 2 h, the radioactivity was determined using a TopCount microplate scintillation counter (PerkinElmer) in the presence of 200 μl of Microscinti-0. LysoPAFAT activity was calculated by subtracting the radioactivity obtained without lyso-PAF from that obtained with lyso-PAF.

PAF-AH assay

PAF-AH activity was evaluated under the same conditions as reported previously, with minor modifications (26, 27). Briefly, 10 μg of protein (100,000 × g supernatant) was incubated at 37 °C for 30 min in a total volume of 0.25 ml of assay buffer (50 mM Tris-HCl (pH 7.4), 5 mM EDTA, 5 mM 2-ME, and 100 μM [*acetyl*-^{3}H]PAF (85 MBq/mmol; PerkinElmer)). The reaction was stopped by adding 2.5 ml of chloroform/methanol (4:1, v/v), followed by 0.25 ml of water. The radioactivity of an aliquot (0.6 ml) of each water phase was measured with 2 ml of the liquid scintillation mixture, Atomlight (PerkinElmer), to determine the amount of acetyl groups liberated from PAF.

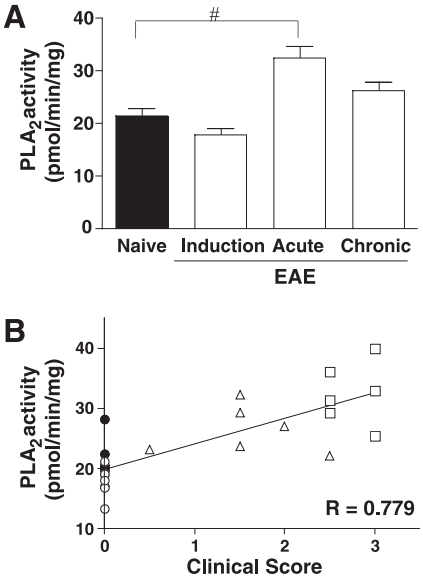

FIGURE 4. PLA_2 activity in SCs of naive and EAE mice. *A*, PLA_2 activity in SCs of naive mice and EAE mice in the induction, acute, and chronic phases ($n = 6$ animals) was measured using mixed micelles containing 1-palmitoyl-2-[^{14}C]arachidonoyl-PC and Triton X-100 in the presence of Ca^{2+} and DTT. Data represent means ± SEM. #, $p < 0.001$ by ANOVA with the Tukey-Kramer test. *B*, PLA_2 activity in naive (●) and EAE mice in the induction (○), acute (□), and chronic (△) phases is positively correlated with the clinical score ($p < 0.0001$ by the Spearman rank correlation test). Each data point represents the result from a single animal.

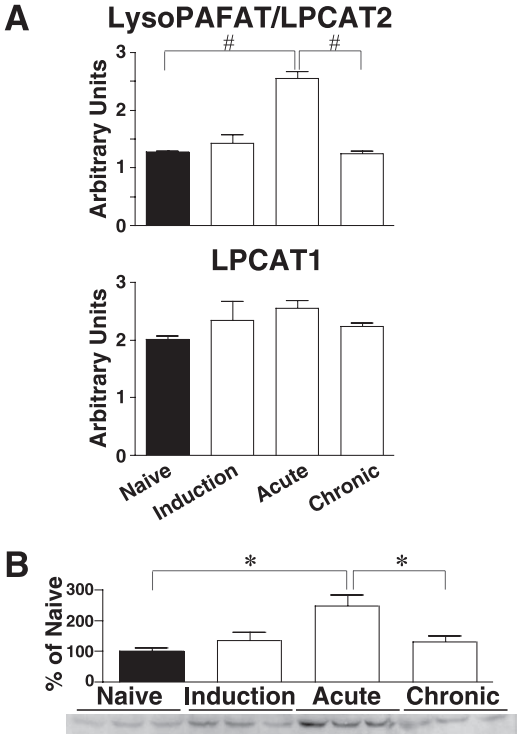

FIGURE 5. LysoPAFAT/LPCAT2 expression in SCs of naive and EAE mice. Expression levels of LysoPAFAT/LPCAT2 and LPCAT1 mRNAs (*A*) and LysoPAFAT/LPCAT2 proteins (*B*) were quantified by real-time PCR and Western blotting with densitometry, respectively, in SCs of naive mice and EAE mice in the induction, acute, and chronic phases ($n = 6$ animals). A representative blot from two independent experiments is shown for LysoPAFAT ($n = 3$ animals). Data represent means ± SEM. #, $p < 0.001$ and ∗, $p < 0.05$ by ANOVA with the Tukey-Kramer test.

Western blotting

Ten micrograms of protein was resolved by 10% SDS-PAGE and transferred to a Hybond ECL nitrocellulose membrane (GE Healthcare Bio-Sciences). The membrane was blocked with 5% skim milk and incubated with anti-LysoPAFAT antiserum (Immuno-Biological Laboratories). After washing, the membranes were incubated with HRP-linked anti-rabbit IgG (GE Healthcare BioSciences), washed, and then exposed to the Western blotting detection reagents (GE Healthcare BioSciences). The membranes were scanned with a LAS-4000 luminescent image analyzer (Fuji film).

Primary culture

Primary young cortical neurons were prepared from C57BL/6 mouse brains on embryonic day 13 as previously described (28, 29). Primary astrocytes and microglia were obtained from cerebral hemispheres of C57BL/6 mouse brains on postnatal day 1, as previously described, with minor modifications (28–30). Briefly, after a 14-day culture period, astrocytes were purified by two passages. Microglia was prepared as a floating cell suspension and transferred to culture dishes. Unattached cells were removed before isolating total RNA. The purities of astrocytes and microglia were estimated to be >90% and >99%, respectively, by immunostaining for glial fibrillary acidic protein (GFAP) and Iba1. Total RNA (1 μg) was reverse-transcribed as described above.

$CD4^+$ and $CD8^+$ T cells were obtained from spleens of C57BL/6 mice using a MACS magnetic cell separation system (Miltenyi Biotec). The purities of $CD4^+$ and $CD8^+$ T cells were estimated to be >90% by flow cytometry (Beckman Coulter). T cells were stimulated with or without anti-CD3ε Ab (BD Biosciences) for 24 h, followed by reverse transcription of total RNA (100 ng) as described above.

Statistical analysis

Results are expressed as means ± SEM. Data were analyzed statistically by means of ANOVA with the Tukey-Kramer post hoc test, the Kruskal-Wallis test with Dunn's post hoc test, or the Spearman rank correlation test as appropriate, using GraphPad PRISM software. Values of $p < 0.05$ were considered to be statistically significant. Cluster analysis was performed using JMP6 software (Hulinks).

Results

Elevation of PAF levels in SCs of EAE mice

C57BL/6 female mice were immunized with $MOG_{35–55}$ and clinical symptoms were monitored (Fig. 2*A*). All mice developed EAE and the mean maximal clinical score was 2.6 ± 0.16 ($n = 8$ animals). To confirm our previous report, PAF levels in SCs were measured by HPLC-ESI-MS/MS. The SCs were collected from naive mice and immunized mice in the induction, acute, and chronic phases of EAE (Fig. 2*A*). PAF levels were significantly elevated in the acute phase (Fig. 2*B*) and positively correlated with the clinical score ($p < 0.0001$; Fig. 2*C*). Thus, the fluctuation in PAF levels during the disease course was reproduced (16). These results demonstrate that the metabolism of PAF (Fig. 1) in the SC was perturbed by the pathogenesis of EAE. Therefore, we determined the enzymes that synthesize and degrade PAF using EAE mice.

Up-regulation of PLA_2 mRNA expression and activity in SCs of EAE mice

The various PLA_2 (groups IVA, IVB, IVC, IVD, IVE, and IVF $cPLA_2$s, groups V and X $sPLA_2$s, and group VI $iPLA_2$) mRNA levels were determined by quantitative RT-PCR to elucidate the effects of PLA_2s on PAF production. Group IVA $cPLA_2$ and group V $sPLA_2$ mRNA levels were elevated in the acute phase of EAE and decreased in the chronic phase to a level that was still higher than that in naive mice (Fig. 3*A*). The relationships among the mRNA levels were evaluated by cluster analysis that distinguished group IVA $cPLA_2$ and group V $sPLA_2$ from other PLA_2s (Fig. 3*B*). In addition, the poorly characterized groups IVB and IVF

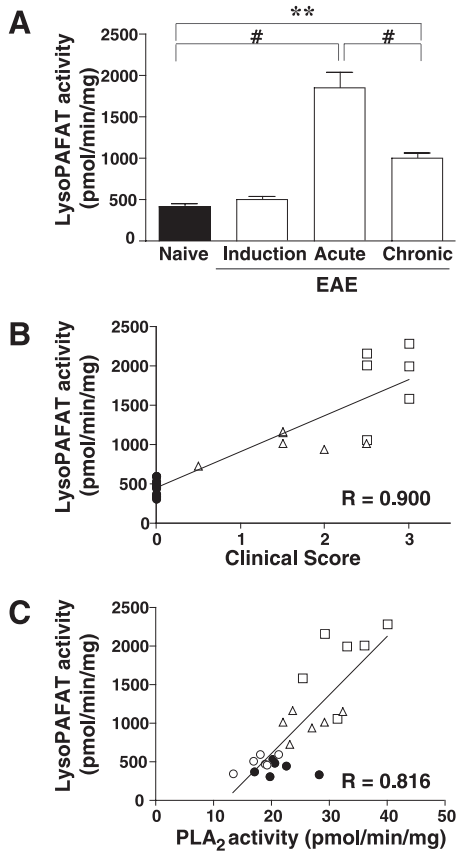

FIGURE 6. LysoPAFAT activity in SCs of naive and EAE mice. *A*, LysoPAFAT activity in SCs of naive mice and EAE mice in the induction, acute, and chronic phases ($n = 6$ animals) was measured as described in *Materials and Methods*. Data represent means ± SEM. #, $p < 0.001$ and **, $p < 0.01$ by ANOVA with the Tukey-Kramer test. *B* and *C*, LysoPAFAT activity in SCs of naive (●) and EAE mice in the induction (○), acute (□), and chronic (△) phases is positively correlated with the clinical score (*B*; $p < 0.0001$ by the Spearman rank correlation test) and PLA_2 activity (*C*; $p < 0.0001$). Each data point represents the results from a single animal.

cPLA$_2$s were up-regulated and clustered together (Fig. 3, *A* and *B*). PLA_2 activity was measured using 1-palmitoyl-2-[^{14}C]arachidonoyl-PC as a substrate with Ca^{2+} and DTT. The enzyme activity increased with the progression of EAE pathology ($p < 0.001$; Fig. 4*A*) and correlated significantly with the clinical score ($p < 0.0001$; Fig. 4B). These results suggest that PAF accumulation in SCs of EAE mice may be due to an up-regulation of PLA_2 and lysoPAFAT (see below).

Enhancement of LysoPAFAT/LPCAT2 expression and activity in SCs of EAE mice

To examine the involvement of LysoPAFAT/LPCAT2, expression levels of the transcripts and proteins were examined in SCs of naive and EAE mice by quantitative RT-PCR and Western blotting, respectively. LysoPAFAT/LPCAT2 transcripts and proteins were elevated in the acute phase and then declined in the chronic phase of EAE (Fig. 5). In contrast, mRNA expression level of the homologous enzyme LPCAT1 was unaltered during the disease course (Fig. 5). In agreement with these observations, the enzyme activities in the acute and chronic phases were higher than those of naive mice ($p < 0.001$; Fig. 6*A*). We found a significantly positive correlation between the clinical score and the LysoPAFAT activity ($p < 0.0001$; Fig. 6*B*). Furthermore, LysoPAFAT activity was

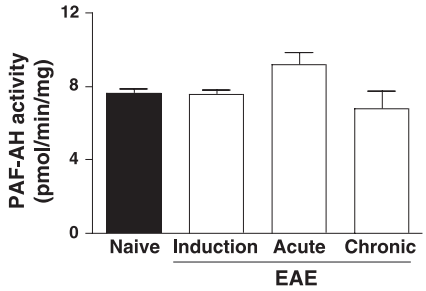

FIGURE 7. PAF-AH activity in SCs of naive and EAE mice. PAF-AH activity in SCs of naive mice and EAE mice in the induction, acute, and chronic phases ($n = 6$ animals) was measured as described in *Materials and Methods*. Data represent means ± SEM.

positively correlated with PLA_2 activity ($p < 0.001$; Fig. 6*C*). These results suggest that PAF accumulation in SCs of EAE mice is caused by the enhancement of LysoPAFAT/LPCAT2 expression and the corresponding increase in LysoPAFAT activity.

Unaltered basal PAF-AH activity in SCs of EAE mice

We investigated whether PAF-AH affected the accumulation of PAF in SCs of EAE mice. Although PAF-AH activity appeared to be slightly increased in the acute phase of EAE, the enzyme activity did not change significantly during the disease course (Fig. 7). PAF-AH activity did not correlate with the clinical score, PLA_2 activity, or LysoPAFAT activity (data not shown). Thus, PAF accumulation in SCs of EAE mice may be independent of the PAF degradation system.

LysoPAFAT/LPCAT2 expression in primary cultured murine microglia and astrocytes

We previously demonstrated LysoPAFAT/LPCAT2 mRNA expression in murine brain, macrophages, and neutrophils (12). Its expression was determined by RT-PCR and Western blotting in primary cultured murine neurons, astrocytes, microglia (Fig. 8), $CD4^+$ T cells, and $CD8^+$ T cells (data not shown). We found that LysoPAFAT/LPCAT2 mRNA was expressed in microglia and astrocytes, but not in neurons (Fig. 8*A*). The levels of LysoPAFAT/LPCAT2 transcripts were very low in both T cell subsets, with or without anti-CD3ε Ab stimulation for 24 h (data not shown). LysoPAFAT/LPCAT2 protein expression was observed in microglia, but not in astrocytes (Fig. 8*B*). These results suggest that PAF may

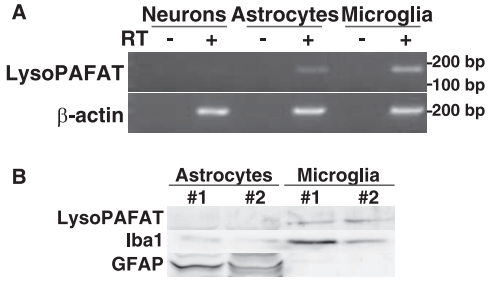

FIGURE 8. LysoPAFAT/LPCAT2 expression in the primary cultured cells of the murine CNS. *A*, LysoPAFAT/LPCAT2 and β-actin mRNA expression in primary cultured neurons, astrocytes, and microglia was determined by RT-PCR. The expected PCR products for LysoPAFAT and β-actin were 167 and 197 bp, respectively. *B*, Expression of LysoPAFAT/LPCAT2, Iba1, and GFAP in primary cultured astrocytes and microglia was determined by Western blotting. Each lane represents cells purified from an individual experiment.

be produced by activated microglia and infiltrating macrophages in SCs of EAE mice.

Discussion

In the present study, we have assessed the metabolic processing of PAF in SCs of naive and EAE mice to explain the enhanced PAF production in EAE mice. In general, accumulation of PAF can be accounted for by the up-regulation of the production system in the remodeling pathway and/or the down-regulation of the degradation system. We have demonstrated that the PAF production system is increased and the degradation system is unchanged in SCs during EAE.

The PAF production system in the remodeling pathway consists of two steps. The first step is production of the PAF precursor lyso-PAF by PLA_2s that hydrolyze the *sn*-2 acyl chain of PC (9) (Fig. 1). Several lines of evidence have suggested that group IVA $cPLA_2$, groups IIA and V $sPLA_2$s, and group VI $iPLA_2$ mRNAs are expressed in the SC of the naive rat (31, 32). In agreement with these studies, we have found that SCs of C57BL/6 mice express these PLA_2 mRNAs, with the exception of group IIA $sPLA_2$ (Fig. 3), which is absent in this mouse strain (33). Because the groups IVA, IVB, and IVF $cPLA_2$s and group V $sPLA_2$ mRNA levels are elevated in the acute phase of EAE (Fig. 3), lipid mediators produced by these four PLA_2s presumably participate in the pathogenesis of EAE. Although little is known about the functions of groups IVB and IVF $cPLA_2$s, it is generally accepted that group IVA $cPLA_2$ and group V $sPLA_2$ stimulate the arachidonic acid cascade (33). Indeed, hierarchical cluster analysis demonstrates the functional analogy of these PLA_2s in EAE pathology (Fig. 3*B*). EAE is not completely ameliorated in PAFR-KO mice (16), whereas group IVA $cPLA_2$ deficiency or treatments with PLA_2 inhibitors protect mice from the EAE pathology (17, 34). Eicosanoid levels were quantified simultaneously and we found that PGE_2 levels were dramatically changed during the disease course (Y. Kihara, S. Ishii, Y. Kita, S. Uematsu, S. Akira, and T. Shimizu, unpublished data). These data suggest that, not only PAF, but also eicosanoids downstream of PLA_2 are critical for the EAE pathology. We have demonstrated the elevation of PLA_2 activity in the acute phase of EAE using 1-palmitoyl-2-[^{14}C]arachidonoyl-PC as a substrate in the presence of Ca^{2+} and DTT (Fig. 4). Since this assay condition is optimized for group IV $cPLA_2$s (35), the elevated PLA_2 activity in the acute phase of EAE may be derived from groups IVA, IVB, and/or IVF $cPLA_2$s. However, groups IVB and IVF $cPLA_2$s have lower PLA_2 activity than group IVA $cPLA_2$ under the present assay conditions (24, 36, 37). Thus, group IVA $cPLA_2$ may be deeply involved in the up-regulation of PLA_2 activity in SCs of EAE mice. Additionally, group IVA $cPLA_2$ is essential for producing PAF, since PAF synthesis is significantly diminished in calcium ionophore-stimulated group IVA $cPLA_2$-deficient macrophages (11). These results suggest that the PAF precursor lyso-PAF is supplied primarily by group IVA $cPLA_2$ during EAE. Because Cunningham et al. (38) reported that $sPLA_2$ activity was up-regulated in urine of EAE rats and MS patients, it may play roles in the EAE pathology. In addition, Bernatchez et al. (39) reported that group V $sPLA_2$ is involved in the PAF production in endothelial cells. Further studies are needed to clarify the roles of group V $sPLA_2$ in EAE lesions.

The second step of the PAF production system is acetylation of lyso-PAF to form PAF by the action of LysoPAFAT, which is critical for the stimulus-dependent formation of PAF (2–4, 12). We have previously shown that LysoPAFAT/LPCAT2 mRNA is expressed in brain, macrophages, and neutrophils (12). Likewise, we have demonstrated the constitutive expression and activity of LysoPAFAT in the SC of naive mice (Figs. 5 and 6). Since LysoPAFAT/LPCAT2 expression is mainly detected in primary cultured microglia by RT-PCR and Western blotting (Fig. 8), microglia may contribute to the production of PAF in the CNS of naive mice for maintaining brain homeostasis (Fig. 9, *left*). A number of inflammatory cells, such as T cells and macrophages, infiltrate the CNS through the broken blood-brain barrier in EAE mice. Furthermore, microglia and astrocytes are activated by cytokines produced by the infiltrating cells (40, 41). The expression and activity of LysoPAFAT were significantly elevated in SCs of EAE mice as compared with those of naive mice (Figs. 5 and 6). Because LysoPAFAT/LPCAT2 is an inducible protein, its expression might be strongly up-regulated in infiltrating macrophages and activated microglia (Fig. 9, *right*). We also have shown that LysoPAFAT activity is correlated with PLA_2 activity (Fig. 6*C*). Kalyvas and David (34) have reported that group IVA $cPLA_2$ is expressed in $CD11b^+$ cells from mice with severe symptoms of EAE. Hence, group IVA $cPLA_2$ and LysoPAFAT appear to be coexpressed in the same cells, such as macrophages/microglia, and to function coordinately in PAF synthesis. In contrast, LysoPAFAT/LPCAT2 mRNA was undetected in T cells stimulation with or without anti-CD3ε Ab for 24 h (data not shown). These results are in accord with previous reports demonstrating that LysoPAFAT activity is present in macrophages (4, 12), but not in T cells (42). The results are also consistent with our previous report that PAF plays a dominant role in the chronic phase of EAE through the activation of macrophages/microglia (16). Taken together, LysoPAFAT induced in macrophages/microglia plays a crucial role in PAF production in EAE pathology (Fig. 9, *right*).

We have measured PAF-AH activity in SCs of naive and EAE mice (Fig. 7) and found that PAF-AH activity is unchanged during the disease course of EAE. Thus, PAF may accumulate in SCs of EAE mice independently of the PAF degradation system.

Our results show that the enzyme activities in the remodeling pathway of PAF synthesis are elevated in SCs of EAE mice due to

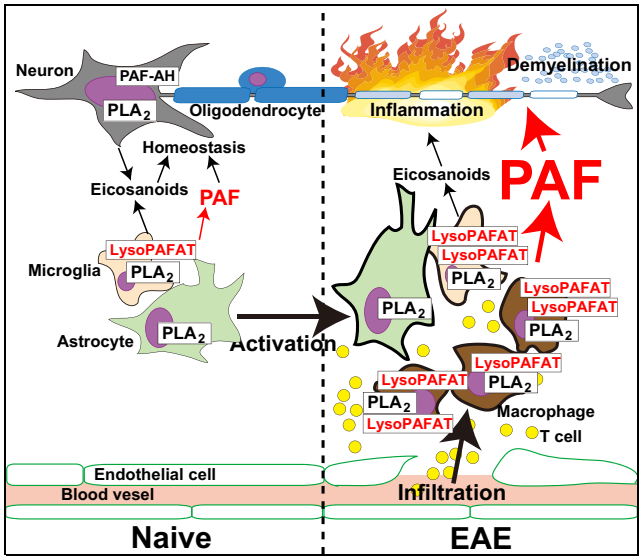

FIGURE 9. Models for PAF production in the CNS of naive mice and EAE mice. *Left*, In the CNS of naive mice, constant levels of PAF produced by microglia and astrocytes may contributes to the maintenance of CNS homeostasis. *Right*, In the CNS of EAE mice, the blood-brain barrier has been broken and inflammatory cells, such as T cells and macrophages, have infiltrated the CNS. LysoPAFAT is induced in activated microglia. Thus, robust PAF production is probably dependent on both LysoPAFAT and group IVA $cPLA_2$ coexpressed in activated macrophages and microglia.

up-regulation of group IVA cPLA$_2$ and LysoPAFAT/LPCAT2 present in macrophages and microglia (Fig. 9). Development of LysoPAFAT inhibitors may be therapeutically beneficial for the treatment of MS.

Acknowledgments

We thank Dr. N. Fukushima (Kinki University, Osaka, Japan) for advising us on the primary culturing of neurons and K. Kuniyeda (University of Tokyo, Tokyo, Japan) for valuable suggestions.

Disclosures

The authors have no financial conflict of interest.

References

1. Ishii, S., and T. Shimizu. 2000. Platelet-activating factor (PAF) receptor and genetically engineered PAF receptor mutant mice. *Prog. Lipid Res.* 39: 41–82.
2. Snyder, F. 1995. Platelet-activating factor: the biosynthetic and catabolic enzymes. *Biochem. J.* 305: 689–705.
3. Shindou, H., S. Ishii, N. Uozumi, and T. Shimizu. 2000. Roles of cytosolic phospholipase A$_2$ and platelet-activating factor receptor in the Ca-induced biosynthesis of PAF. *Biochem. Biophys. Res. Commun.* 271: 812–817.
4. Shindou, H., S. Ishii, M. Yamamoto, K. Takeda, S. Akira, and T. Shimizu. 2005. Priming effect of lipopolysaccharide on acetyl-coenzyme A:lyso-platelet-activating factor acetyltransferase is MyD88 and TRIF independent. *J. Immunol.* 175: 1177–1183.
5. Owen, J. S., P. R. Baker, J. T. O'Flaherty, M. J. Thomas, M. P. Samuel, R. E. Wooten, and R. L. Wykle. 2005. Stress-induced platelet-activating factor synthesis in human neutrophils. *Biochim. Biophys. Acta* 1733: 120–129.
6. Honda, Z., M. Nakamura, I. Miki, M. Minami, T. Watanabe, Y. Seyama, H. Okado, H. Toh, K. Ito, T. Miyamoto, and T. Shimizu. 1991. Cloning by functional expression of platelet-activating factor receptor from guinea-pig lung. *Nature* 349: 342–346.
7. Arai, H., H. Koizumi, J. Aoki, and K. Inoue. 2002. Platelet-activating factor acetylhydrolase (PAF-AH). *J. Biochem.* 131: 635–640.
8. Kudo, I., and M. Murakami. 2002. Phospholipase A$_2$ enzymes. *Prostaglandins Other Lipid Mediat.* 68–69: 3–58.
9. Kita, Y., T. Ohto, N. Uozumi, and T. Shimizu. 2006. Biochemical properties and pathophysiological roles of cytosolic phospholipase A2s. *Biochim. Biophys. Acta* 1761: 1317–1322.
10. Funk, C. D. 2001. Prostaglandins and leukotrienes: advances in eicosanoid biology. *Science* 294: 1871–1875.
11. Uozumi, N., K. Kume, T. Nagase, N. Nakatani, S. Ishii, F. Tashiro, Y. Komagata, K. Maki, K. Ikuta, Y. Ouchi, et al. 1997. Role of cytosolic phospholipase A2 in allergic response and parturition. *Nature* 390: 618–622.
12. Shindou, H., D. Hishikawa, H. Nakanishi, T. Harayama, S. Ishii, R. Taguchi, and T. Shimizu. 2007. A single enzyme catalyzes both platelet-activating factor production and membrane biogenesis of inflammatory cells: cloning and characterization of acetyl-CoA:LYSO-PAF acetyltransferase. *J. Biol. Chem.* 282: 6532–6539.
13. Pedotti, R., J. J. De Voss, L. Steinman, and S. J. Galli. 2003. Involvement of both "allergic" and "autoimmune" mechanisms in EAE, MS and other autoimmune diseases. *Trends Immunol.* 24: 479–484.
14. Steinman, L., and S. S. Zamvil. 2006. How to successfully apply animal studies in experimental allergic encephalomyelitis to research on multiple sclerosis. *Ann. Neurol.* 60: 12–21.
15. Howat, D. W., N. Chand, P. Braquet, and D. A. Willoughby. 1989. An investigation into the possible involvement of platelet activating factor in experimental allergic encephalomyelitis in rats. *Agents Actions* 27: 473–476.
16. Kihara, Y., S. Ishii, Y. Kita, A. Toda, A. Shimada, and T. Shimizu. 2005. Dual phase regulation of experimental allergic encephalomyelitis by platelet-activating factor. *J. Exp. Med.* 202: 853–863.
17. Marusic, S., M. W. Leach, J. W. Pelker, M. L. Azoitei, N. Uozumi, J. Cui, M. W. Shen, C. M. DeClercq, J. S. Miyashiro, B. A. Carito, et al. 2005. Cytosolic phospholipase A2 α-deficient mice are resistant to experimental autoimmune encephalomyelitis. *J. Exp. Med.* 202: 841–851.
18. Callea, L., M. Arese, A. Orlandini, C. Bargnani, A. Priori, and F. Bussolino. 1999. Platelet activating factor is elevated in cerebral spinal fluid and plasma of patients with relapsing-remitting multiple sclerosis. *J. Neuroimmunol.* 94: 212–221.
19. Lock, C., G. Hermans, R. Pedotti, A. Brendolan, E. Schadt, H. Garren, A. Langer-Gould, S. Strober, B. Cannella, J. Allard, et al. 2002. Gene-microarray analysis of multiple sclerosis lesions yields new targets validated in autoimmune encephalomyelitis. *Nat. Med.* 8: 500–508.
20. Pedotti, R., J. J. DeVoss, S. Youssef, D. Mitchell, J. Wedemeyer, R. Madanat, H. Garren, P. Fontoura, M. Tsai, S. J. Galli, et al. 2003. Multiple elements of the allergic arm of the immune response modulate autoimmune demyelination. *Proc. Natl. Acad. Sci. USA* 100: 1867–1872.
21. Kita, Y., T. Takahashi, N. Uozumi, L. Nallan, M. H. Gelb, and T. Shimizu. 2005. Pathway-oriented profiling of lipid mediators in macrophages. *Biochem. Biophys. Res. Commun.* 330: 898–906.
22. Kita, Y., T. Takahashi, N. Uozumi, and T. Shimizu. 2005. A multiplex quantitation method for eicosanoids and platelet-activating factor using column-switching reversed-phase liquid chromatography-tandem mass spectrometry. *Anal. Biochem.* 342: 134–143.
23. Nakanishi, H., H. Shindou, D. Hishikawa, T. Harayama, R. Ogasawara, A. Suwabe, R. Taguchi, and T. Shimizu. 2006. Cloning and characterization of mouse lung-type acyl-CoA:lysophosphatidylcholine acyltransferase 1 (LPCAT1): expression in alveolar type II cells and possible involvement in surfactant production. *J. Biol. Chem.* 281: 20140–20147.
24. Ohto, T., N. Uozumi, T. Hirabayashi, and T. Shimizu. 2005. Identification of novel cytosolic phospholipase A$_2$s, murine cPLA$_2\delta$, ε, and ζ, which form a gene cluster with cPLA$_2\beta$. *J. Biol. Chem.* 280: 24576–24583.
25. Kume, K., I. Waga, and T. Shimizu. 1997. Microplate chromatography assay for acetyl-CoA: lysoplatelet-activating factor acetyltransferase. *Anal. Biochem.* 246: 118–122.
26. Hattori, K., M. Hattori, H. Adachi, M. Tsujimoto, H. Arai, and K. Inoue. 1995. Purification and characterization of platelet-activating factor acetylhydrolase II from bovine liver cytosol. *J. Biol. Chem.* 270: 22308–22313.
27. Ohshima, N., S. Ishii, T. Izumi, and T. Shimizu. 2002. Receptor-dependent metabolism of platelet-activating factor in murine macrophages. *J. Biol. Chem.* 277: 9722–9727.
28. Mori, M., M. Aihara, K. Kume, M. Hamanoue, S. Kohsaka, and T. Shimizu. 1996. Predominant expression of platelet-activating factor receptor in the rat brain microglia. *J. Neurosci.* 16: 3590–3600.
29. Aihara, M., S. Ishii, K. Kume, and T. Shimizu. 2000. Interaction between neurone and microglia mediated by platelet-activating factor. *Genes Cells* 5: 397–406.
30. Tabuchi, S., K. Kume, M. Aihara, and T. Shimizu. 2000. Expression of lysophosphatidic acid receptor in rat astrocytes: mitogenic effect and expression of neurotrophic genes. *Neurochem. Res.* 25: 573–582.
31. Lucas, K. K., C. I. Svensson, X. Y. Hua, T. L. Yaksh, and E. A. Dennis. 2005. Spinal phospholipase A2 in inflammatory hyperalgesia: role of group IVA cPLA2. *Br. J. Pharmacol.* 144: 940–952.
32. Svensson, C. I., K. K. Lucas, X. Y. Hua, H. C. Powell, E. A. Dennis, and T. L. Yaksh. 2005. Spinal phospholipase A$_2$ in inflammatory hyperalgesia: role of the small, secretory phospholipase A$_2$. *Neuroscience* 133: 543–553.
33. Murakami, M., and I. Kudo. 2002. Phospholipase A$_2$. *J. Biochem.* 131: 285–292.
34. Kalyvas, A., and S. David. 2004. Cytosolic phospholipase A$_2$ plays a key role in the pathogenesis of multiple sclerosis-like disease. *Neuron* 41: 323–335.
35. Lucas, K. K., and E. A. Dennis. 2005. Distinguishing phospholipase A$_2$ types in biological samples by employing group-specific assays in the presence of inhibitors. *Prostaglandins Other Lipid Mediat.* 77: 235–248.
36. Pickard, R. T., B. A. Strifler, R. M. Kramer, and J. D. Sharp. 1999. Molecular cloning of two new human paralogs of 85-kDa cytosolic phospholipase A$_2$. *J. Biol. Chem.* 274: 8823–8831.
37. Song, C., X. J. Chang, K. M. Bean, M. S. Proia, J. L. Knopf, and R. W. Kriz. 1999. Molecular characterization of cytosolic phospholipase A$_2$-β. *J. Biol. Chem.* 274: 17063–17067.
38. Cunningham, T. J., L. Yao, M. Oetinger, L. Cort, E. P. Blankenhorn, and J. I. Greenstein. 2006. Secreted phospholipase A$_2$ activity in experimental autoimmune encephalomyelitis and multiple sclerosis. *J. Neuroinflammation* 3: 26.
39. Bernatchez, P. N., M. V. Winstead, E. A. Dennis, and M. G. Sirois. 2001. VEGF stimulation of endothelial cell PAF synthesis is mediated by group V 14 kDa secretory phospholipase A$_2$. *Br. J. Pharmacol.* 134: 197–205.
40. Benveniste, E. N. 1997. Role of macrophages/microglia in multiple sclerosis and experimental allergic encephalomyelitis. *J. Mol. Med.* 75: 165–173.
41. Bannerman, P., A. Hahn, A. Soulika, V. Gallo, and D. Pleasure. 2007. Astrogliosis in EAE spinal cord: derivation from radial glia, and relationships to oligodendroglia. *Glia* 55: 57–64.
42. Garcia, M. C., C. Garcia, M. A. Gijon, S. Fernandez-Gallardo, F. Mollinedo, and M. Sanchez Crespo. 1991. Metabolism of platelet-activating factor in human haematopoietic cell lines: differences between myeloid and lymphoid cells. *Biochem. J.* 273: 573–578.